ANALYSIS OF FLOOD-AFFECTED AREAS DUE TO EXTREME WEATHER IN PACITAN, INDONESIA

*Muhammad Musiyam[1,3], Jumadi Jumadi[1,2], Yunus Aris Wibowo[1,3], Wahyu Widiyatmoko[1,3] and Siti Hadiyati Nur Hafida[1,3]

[1]Centre for Disaster Mitigation Study, Universitas Muhammadiyah Surakarta, Indonesia
[2]Faculty of Geography, Universitas Muhammadiyah Surakarta, Indonesia
[3]Department of Geography Education, Faculty of Teacher Training and Education (FKIP), Universitas Muhammadiyah Surakarta, Indonesia

ABSTRACT: Extreme weather events such as tropical cyclones trigger floods in parts of Indonesia and result in massive damage. Tropical Cyclone Cempaka in 2017 is an example of such an event, which caused high levels of loss of life and property in Pacitan Regency. This area is located in the southern part of Java Island, an area prone to tropical cyclones. This paper aims to identify the specific area of Pacitan, Indonesia, that is affected to flood hazards triggered by extreme weather. The flood event during Cyclone Cempaka in 2017 is used as a case study, and the identification of flood-affected areas due to extreme weather was carried out by an analysis of Landsat 8 satellite imagery. Normalized Differentiation Vegetation Index (NDVI) was used to identify the inundated areas at that time, corrected by Normalized Difference Water Index (NDWI), slope, and landform. The flood-affected area included 11 villages with a total area of 412.684 hectares. Those villages are located in areas of landform resulting from fluvial processes with slope 0-2 and 2-7% which are prone to flooding. The results of the identification are appropriate for preparing mitigation strategies for the area.

Keywords: flood hazard, extreme weather, tropical cyclone, remote sensing, GIS

1. INTRODUCTION

Extreme weather is defined as unpredictable, unusual, severe or unseasonal weather at the extreme of historical distribution. In recent years, much evidence indicates that global warming caused by human activity increases the periodicity and intensity of some extreme weather events [1-4]. These events have a significant influence on human society [5,6] and on natural ecosystems [7,8]. Tropical cyclones are among the extreme weather events experienced in Indonesia.

Tropical cyclones (or typhoons) are events that have the potential to harm human populations [9-12]. From a meteorological perspective, the term 'tropical cyclone' refers to the formation of low pressure that generally occurs in the tropics at latitudes between 10⁰ and 20⁰ South/North of the equator [8-13]. Tropical cyclones occur in the Earth's atmosphere above warm seas located in the tropics and play an important role in heat transfer from low to higher latitudes [14,15]. Geographically, Indonesia is not in a tropical cyclone track and does not meet the regional requirements for cyclone formation; however, although tropical cyclones never actually occur in Indonesia, their effects are often felt there.

The impact of tropical cyclones can reach for thousands of kilometres from the centre of the storm and cause heavy rain and strong winds leading to flooding, landslides, falling trees and danger to aircraft and shipping [16-18]. Since 1983 there have been nine cyclone events around Indonesian waters that have affected the weather in parts of Indonesia [19]. Of these, Cyclone Cempaka occurred closest to Indonesian territory, with impacts on weather such as heavy rains, strong winds, and storms triggering natural disasters such as flooding, flash floods, and landslides [10,19,20]. Areas affected by Cyclone Cempaka included Jakarta, West Java, Central Java, Yogyakarta Special Region, East Java, Kangean Island, Bali, Nusa Tenggara, and southern Java waters.

One of the areas affected by Cyclone Cempaka that suffered a very large amount of damage and loss resulting from extreme rainfall was Pacitan Regency and surrounding areas, East Java. Monthly rainfall in Pacitan Regency for November between 1987 and 2006 was in the range of 110 mm to 125 mm, but during Cyclone Cempaka, November rainfall increased dramatically, to between 800 mm and 950 mm across the area [21]. The high intensity of this rainfall triggered various disasters in several regions of Indonesia, and especially in East Java.

The region of South Java is prone to various types of natural disasters [22]. The Pacitan Regency is one of the areas of southern Java that was closest to Cyclone Cempaka, and weather changes that occurred were extreme and caused floods and landslides in several locations. The disaster resulted

in 25 fatalities, approximately 4,000 people were affected and evacuated, and material losses to infrastructure and settlements and economic, cultural, and other cross-sectoral losses reached Rp 1 trillion [23]. In light of impacts such as these, efforts are needed to identify the total area affected by flooding and to take appropriate disaster-mitigation measures to reduce the risk of loss during future disasters.

One of the efforts made to identify areas affected by floods in Pacitan is the use of remote-sensing technology for tentative analysis of the affected area. The data gathered can then be further corrected with other supporting data. This study focuses on the identification of flood-affected areas triggered by Cyclone Cempaka in 2017. The location of the study area is Arjosari District, Pacitan Regency. The location was chosen because it has been repeatedly hit by floods and has high population numbers (41,686) and density (356 people / km^2) [24]. Identification of the affected area is very important as an assessment of damage and losses, and in devising mitigation plans to reduce the impact of future disasters [25].

Remote-sensing technology was chosen as the basis for this data analysis because it offers results that can be scientifically justified and are relatively cost-effective to obtain [3]. This technology is therefore very suitable for preliminary studies. This preliminary study is an initial step in a series of studies in the same area, results of which can be used as a basis for further research and are relevant for use in decision making and planning for appropriate disaster mitigation.

2. METHOD

This study was conducted in part of Arjosari Subdistrict, Pacitan Regency, East Java Province (Fig.1). The location of the study was determined by conducting a literature study of the area affected by floods triggered by Cyclone Cempeka. Literature study data are tabular and descriptive and so spatial studies need to be carried out in order to spatially identify the area affected by floods that were triggered by Cyclone Cempaka.

Even though the number of villages/*kelurahan* (village offices) affected by flooding in Arjosari Subdistrict is not as high as in other subdistricts, this district was chosen because of its relatively frequent flooding events compared to other areas, whether due to river overflow or triggered by cyclone phenomena. After determining the location of the study, satellite images that covers Arjosari District were selected.

The next step is the selection of the satellite imagery that is suitable for the analysis technique and the purpose of the study. The satellite imagery used in this study is Landsat 8 imagery from 5

December 2017 obtained from the website http://earthexplorer.usgs.gov [26]. Landsat 8 imagery has a temporal resolution of 16 days and images were selected with recording date closest to the Cempaka tropical cyclone event. It was chosen because the recording time is close to the time of the flood disaster triggered by Cyclone Cempaka and the visual quality of the image is only slightly distorted. The image was then processed and analysed to obtain Normalized Differentiation Vegetation Index (NDVI) data, this being the most commonly used vegetation index [27]. This index is obtained by utilizing the red and near-infrared channels, both of which have a fairly large range of responses to vegetation, making it easier to distinguish between wet and dry areas [28]. The formula used for NDVI analysis is presented in Eq. (1).
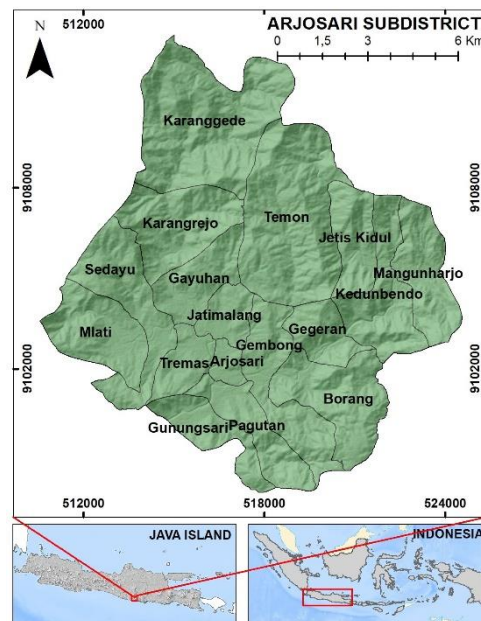

Fig.1 The Study Area.

$$NDVI = (NIR - Red) / (NIR + Red) \qquad (1)$$

Remote sensing technology such as NDVI has long been used for the analysis of flood-affected areas. [29] use a Modified Normalized Divergence Water Index (MNDWI) utilizing Landsat 5 Thematic Mapper (L5-TM) images and Landsat 8 Operational Land Imager (L8-OLI) to identify wetlands in the Ramsar Wetlands Reserve, Argentina. Meanwhile, [30] use more complex methods to assess the danger of flash floods in the Haraz river basin, North Iran; these methods include Logistic Model Trees (LMT), Reduced Error Pruning Trees (REPT), Naive Bayes Trees (NBT) and Alternating Decision Trees (ADT), which utilise data relating to ground slope, altitude, curvature, Stream Power Index (SPI), Topographic

Wetness Index (TWI), land use, rainfall, river density, distance from river, lithology and NDVI. Furthermore, [31] designed a flood scenario using RADARSAT and MODIS data for flood mapping in Thailand. However, slightly different from some of these studies, this study seeks to analyze flood-affected areas due to extreme weather by using NDVI responses to various types of land cover

In this study, the interpretation of flooded areas is based on the identification of elements of image interpretation, namely hue and colour [32]. Areas with darker hues and blacker colours than other areas were identified as being flooded at the time of recording. Flooded areas will appear darker because water absorbs almost all wavelengths, so that water in the image will look dark. The assumption used in this study is that wet areas are areas that are affected by floods and areas that tend to be dry are not affected by floods. Corrections are performed using hydrographic data, slope data, landforms and land-use data from colour panchromatic images to distinguish between flooded areas and water bodies or wet agricultural areas.

Hydrographic data is obtained from the interpretation of three-dimensional topographic data and uses hydrographic data from Indonesian land maps published by the Geospatial Information Agency (BIG). The slope and dimensional shape data used is the result of processing the National Digital Elevation Model (DEMNAS) data obtained from http://tides.big.go.id/DEMNAS/ [33]. The next step is the delineation of areas affected by the flooding triggered by Cyclone Cempaka.

3. RESULTS AND DISCUSSION

3.1 Imagery Selection and Normalized Differentiation Vegetation Index (NDVI) Analysis

The selection of satellite imagery was carried out after determining the study area. The study area was determined based on data from the National Disaster Management Agency (BNPB). Data is presented for the three locations most severely affected by Cyclone Cempaka in Pacitan District in 2017 (Table 1).

Arjosari Subdistrict was chosen with consideration to several villages in the region which had repeatedly experienced flooding. The data is analysed in accordance with the administrative boundaries of Arjosari District and the Landsat 8 imagery was cut in accordance with the district boundary. Image cutting aims to ensure the image to be processed is specific to the area to be studied and in accordance with the region of interest.

Table 1 Cyclone Cempaka-affected areas in Pacitan Regency, 2017

No	Subdistricts	Villages
1.	Pacitan	Sirnoboyo, Sukoharjo, Kayen, Kembang, Ploso, Arjowinangun, Sidoharjo
2.	Kebon Agung	Purworejo, Banjarjo, Kebon Agung
3.	Arjosari	Pagutan, Jatimalang, Arjosari, Tremas

This study focuses on the utilization of NDVI results from Landsat 8 data processing which is corrected by the characteristics of the research area. NDVI utilizes the functions of two image bands, namely the red band (RED) and the near-infrared band (NIR) and produces a range of values from -1 to 1. After NDVI is obtained, the next step is to match the results of the NDVI analysis with the 1986 Holben classification [34] (Table 2). The classification is made with the aim of distinguishing between vegetation and other objects such as clouds, bare soil, rocks and surface water. Therefore, this study uses these classifications as initial identification, with the assumption that flood-affected areas can be identified from areas with values according with water criteria.

Table 2 Classification of NDVI for various types of land cover

No.	Cover type	RED	NIR	NDVI
1.	Dense green-leaf vegetation	0.050	0.150	0.500
2.	Medium green-leaf vegetation	0.080	0.110	0.140
3.	Light green-leaf vegetation	0.100	0.120	0.090
4.	Bare soil	0.269	0.283	0.025
5.	Clouds (opaque)	0.227	0.228	0.002
6.	Snow and ice	0.375	0.342	-0.046
7.	Water	0.022	0.013	-0.257

Source: Holben, 1986

The results of the analysis show that the area identified as flooded includes areas with values below 0. These areas are included in 11 administrative areas of villages in the Arjosari District, Pacitan Regency (Fig.2). These areas appear darker than the surrounding area because it is wetter, so it can be assumed that the area is flooded.
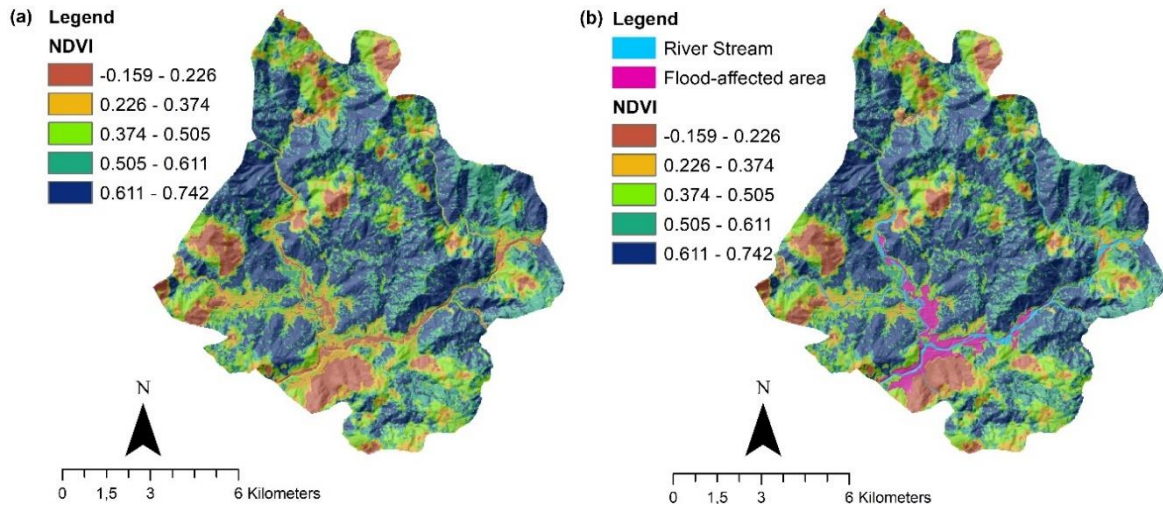
Fig.2 NDVI as initial factor used to derive flood-affected area. (a) NDVI, (b) NDVI overlaid with stream networks and flood affected areas.

The use of remote sensing technology has long been developed for the analysis of flood-affected areas as well as analysis of losses due to flooding. [35] utilizing SRTM, and Landsat imagery combined with land use data, slope, and hydrological data for the analysis of flash flood affected-areas. The resulting maps produce a high level of accuracy because the use of remote sensing data is also supported by topography and hydrology data. Furthermore, the combination of analysis between remote sensing technology and hydrological modeling is often used by researchers. It can produce a good quality of spatial distribution of flood-affected areas because they used various types of data. Such research was carried out by [36-38] for the analysis of flood-affected areas and the potential losses caused by it. However, the large amount of data used in these studies sometimes

becomes a barrier in researching due to high costs. Therefore, this study seeks to show that the use of relatively inexpensive data and simple analysis can produce the distribution of flood-affected areas with good accuracy even on a small scale.

3.2 Identification of Slope and Landform

Topographic data is used as a comparison as well as for corrections to landform data. The landform analysis conducted is interpretation at the macro scale, which only identifies landforms based on their morphology and morphogenes on a small scale. The more accurate the topographic data used, the better the correction results become [39]. The results of identification show that Arjosari Subdistrict consists of two principle landforms, namely those resulting from the denudational process and those resulting from fluvial processes.
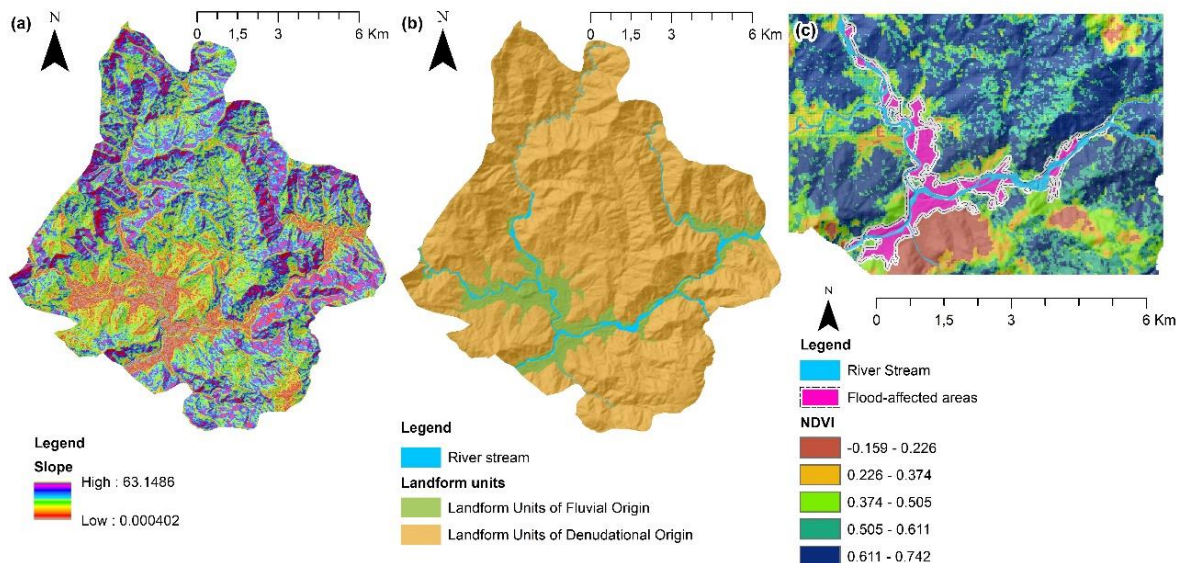

Fig.3 The controlling and correction factors used to derive flood-affected area. (a) Slope and (b) landform, (c) flood-affected area compared with slope and landform units.

The area affected by floods triggered by Cyclone Cempaka is located in areas of landform resulting from fluvial processes. If analysed further, these landforms are found to comprise the valley between hills associated with the Grindulu and Asemgondok river flows, so that can be seen to be the area prone to flood events [28].

Other topographic data used relate to the slope. Although the slope aspect is one of the main aspects of landforms, in this study, the data is distinguished of flood-affected areas according to the characteristics of the region as conducted by [40,41]. Furthermore, the geomorphological approach carried out by [42-44] is not only able to present the flood-affected areas spatially able to present the results of flood mitigation planning as well. The data used in these studies were obtained from processing the Shuttle Radar Topographic Mission (SRTM), geological map, Landsat 8 imagery, hydroclimatic, and streamflow measurements. Indeed, the geomorphological approach in flood studies cannot be separated from remote sensing technology. The combination between geomorphological approach and remote sensing can be conducted in a complex manner or comparing geomorphological elements such as slope and elevation. This study uses a partial geomorphological approach, namely identification of landforms and slope to test the accuracy of flood-affected areas based on the results of Landsat 8 imagery interpretation (Fig.3). The advantage of the partial approach is that the characteristics of the flood-affected area can be more exposed so that it can be the basis for further studies.

3.3 Discussion

Corrections to the identification of flood-affected areas are carried out by overlapping the flood-affected areas drawn from NDVI interpretation with landform and slope maps [43]. The results of the intercropping show that the results of identification of NDVI-based flooded areas in Arjosari Subdistrict are quite accurate because the characteristics of the slopes and the shape of the area affected by the flood are identical and have characteristics prone to flooding (Table 3).

The flood-affected area analysis can be conducted by using both 1D and 2D hydrological modeling. The details of the DEM data greatly affect the accuracy of the resulting model [45]. DEM data used in modeling are generally in the form of raster or Triangulated Irregular Network (TIN), while for simple analysis using manual delineation in the form of shaded relief.

The type of data and the quality of the data will affect the results of the analysis conducted both underestimate and overestimate results [46]. DEM data that are ideal for flood mapping should have an accuracy of less than 1 meter because it can cover flood height differences that vary from the smallest interval [47]. Using a high-quality data and choosing an appropriate flood analysis will result in an accurate spatial distribution of flood-affected areas [48,49]. Furthermore, the use of simpler technology, both automatic and manual with 3D Analyst and Spatial Analyst tools tends to overestimate [46].

Table 3 Flood-affected area correction compared with slope and landform units

Village	Landform (slope)_	Material	Flooded (ha)
Kedungbendo			0.7
Gayuhan			34.5
Jatimalang			35.9
Gembong	Fluvial origin (0–2, 2–7)	Alluvium, cobble, pebble, sand, silt, clay, mud	46.2
Gegeran			24.6
Tremas			17.7
Arjosari			79.3
Borang			46.6
Karangrejo			3.2
Pagutan			57.4
Gunungsari			66.1
Total			412.684

However, the results of the analysis can still be considered for both academic and practical purposes. This study does use very simple technology for the analysis of flood-affected areas. Therefore, the correction is done not only using topographic data from the DEM but also using slope and landform data. Also, the identification of river flow connectivity was carried out to strengthen the analysis [50]. Correction using topographic data, especially slopes, supported by landform data in this study, produced a fairly good flood-affected area map.

Moreover, the results of this study can be used as a basis for disaster mapping or risk assessment. Correction using slope and landform data is performed as a control because in this study the identification of flood-affected areas is only based on the results of NDVI analysis without using NDWI data.

4. CONCLUSION

The mapping of flood-affected areas, especially those triggered by Cyclone Cempaka, is important as a baseline so that appropriate mitigation plans can be put in place for future disaster events. The analysis result shows that all 11 villages affected by flooding due to extreme weather in the Arjosari sub-

district possess characteristics that are prone to flooding. Based on the topographical conditions, the area of these villages is in the inter-hilly valley area that is crossed by the Grindulu River and Asemgondok. Moreover, the landform that dominates these villages is the fluvial origin that is identical to the flood; not to mention, another characteristic which is also very essential is the slope, it is relatively flat with a small height difference so it is prone to flooding. The identification of flood-affected areas triggered by Cyclone Cempaka based on NDVI data controlled and corrected using landform and slope data shows optimal results in maps. It is feasible to use because the identification results are not only based on remote-sensing data but also use data for the physical characteristics of the affected areas. These results are used as a preliminary study for the identification of flood hazards and analysis of flood risks and to estimate losses due to flood disasters in Pacitan Regency.

5. ACKNOWLEDGMENTS

6. REFERENCES

[1] Haque U., da Silva P.F., Devoli G., Pilz J., Zhao B., Khalouah A., Wilopo W., Andersen P., Lu P., Lee J., Yamamoto T., Keellings D., Jian-Hong W., and Glass G.E., "The human cost of global warming: Deadly landslides and their triggers (1995–2014)," *Sci. Total Environ.*, vol. 682, 2019, pp.673-684, doi: 10.1016/j.scitotenv.2019.03.415.

[2] Wang Z., Liu J., Xu N., Fan C., Fan Y., He S., Jiao L., and Ma N., "The role of indigenous knowledge in integrating scientific and indigenous knowledge for community-based disaster risk reduction: A case of Haikou Village in Ningxia, China," *Int. J. Disaster Risk Reduct.*, vol. 41, 2019, doi: 10.1016/j.ijdrr.2019.101309.

[3] Wu K.S., He Y.R., Chen Q.J., and Zheng Y.M., "Analysis on the damage and recovery of typhoon disaster based on UAV orthograph," *Microelectron. Reliab.*, vol. 107, no. May 2019, 2020, p.113337, doi: 10.1016/j.microrel.2019.06.029.

[4] Doornkamp J.C., "Coastal flooding, global warming and environmental management," *J. Environ. Manage.*, vol. 52, no. 4, 1998, pp.327-333, doi: 10.1006/jema.1998.0188.

[5] Chou J., Dong W., Tu G., and Xu Y., "Spatiotemporal distribution of landing tropical cyclones and disaster impact analysis in coastal China during 1990–2016," *Phys.*

Chem. Earth, vol. 115, 2020, p.102830, doi: 10.1016/j.pce.2019.102830.

[6] Li L., Xiao Y., Zhou H., Xing F., and Song L., "Turbulent wind characteristics in typhoon Hagupit based on field measurements," *Int. J. Distrib. Sens. Networks*, vol. 14, no. 10, 2018, doi: 10.1177/1550147718805934.

[7] Djalante R., "Key assessments from the IPCC special report on global warming of 1.5 °C and the implications for the Sendai framework for disaster risk reduction," *Prog. Disaster Sci.*, vol. 1, no. February, 2019, p.100001, doi: 10.1016/j.pdisas.2019.100001.

[8] Hoque M.A.A., Phinn S., and Roelfsema C., "A systematic review of tropical cyclone disaster management research using remote sensing and spatial analysis," *Ocean Coast. Manag.*, vol. 146, 2017, pp.109-120, doi: 10.1016/j.ocecoaman.2017.07.001.

[9] Henderson-Sellers A., "Tropical cyclone and global climate change: A post IPCC assessment," *Bull. Am. Meteorol. Soc.*, vol. Vol. 79, 1998, pp.19-38.

[10] Ren D., and Leslie L.M., "Changes in tropical cyclone activity over Northwest Western Australia in the past 50 years and a view of the future 50 years," *Earth Interact.*, vol. 19, no. 15, 2015, doi: 10.1175/EI-D-14-0006.1.

[11] Liu Y.C., Chen H.F., Liu X., and Chang Y.P., "Insight into tropical cyclone behaviour through examining maritime disasters over the past 1000 years based on the dynastic histories of China – A dedication to Ocean Researcher V," *Quat. Int.*, vol. 440, 2017, pp.72-81, doi: 10.1016/j.quaint.2016.05.025.

[12] Mansour S., "Geospatial modelling of tropical cyclone risks to the southern Oman coasts," *Int. J. Disaster Risk Reduct.*, vol. 40, no. January, 2019, p. 101151, doi: 10.1016/j.ijdrr.2019.101151.

[13] Wang L., Zhou Y., Lei X., Zhou Y., Bi H., and Mao X., "Predominant factors of disaster caused by tropical cyclones in South China coast and implications for early warning systems," *Sci. Total Environ.*, 2019, p.183135, doi:https://doi.org/10.1016/j.scitotenv.2020.138556.

[14] Aminatun S., and Anggraheni D., "Pengaruh Badai Tropis Cempaka Terhadap Kejadian Tanah Longsor di Kabupaten Bantul Yogyakarta," *J. Teknol. Rekayasa*, vol. 3, no. 1, 2018, p.105, doi: 10.31544/jtera.v3.i1.2018.105-114.

[15] Pal I., Ghosh T., and Ghosh C., "Institutional framework and administrative systems for effective disaster risk governance – Perspectives of 2013 Cyclone Phailin in India," *Int. J. Disaster Risk Reduct.*, vol. 21, 2017, pp.350-359, doi: 10.1016/j.ijdrr.2017.01.002.

[16] Varotsos C.A., Krapivin V.F., and Soldatov V.Y., "Monitoring and forecasting of tropical cyclones: A new information-modeling tool to reduce the risk," *Int. J. Disaster Risk Reduct.*, vol. 36, no. January, 2019, p.101088, doi: 10.1016/j.ijdrr.2019.101088.

[17] R Mind'je R., Li L., Amanambu A.C., Nahayo L., Nsengiyumva J.B., Gasirabo A., and Mindje M., "Flood susceptibility modeling and hazard perception in Rwanda," *Int. J. Disaster Risk Reduct.*, vol. 38, no. April 2018, 2019, p.101211, doi: 10.1016/j.ijdrr.2019.101211.

[18] Chhotray V., and Few R., "Post-disaster recovery and ongoing vulnerability: Ten years after the super-cyclone of 1999 in Orissa, India," *Glob. Environ. Chang.*, vol. 22, no. 3, 2012, pp.695-702, doi: 10.1016/j.gloenvcha.2012.05.001.

[19] Mulyana E., Bayu M., Prayoga R., Yananto A., Wirahma S., Aldrian E., Harsoyo B., Seto T.H., and Sunarya Y., "Tropical cyclones characteristic in southern Indonesia and The impact on extreme rainfall event," in *MATEC Web of Conference*, 2018.

[20] Hoque M.A.A., Phinn S., Roelfsema C., and Childs I., "Assessing tropical cyclone risks using geospatial techniques," *Appl. Geogr.*, vol. 98, no. March 2017, 2018, pp.22-33, doi: 10.1016/j.apgeog.2018.07.004.

[21] Putro D.A., "Cempaka, Dahlia lalu Eceng Gondok?," *Waspada Catastrophe Newsletter*, 2018, pp.6-14.

[22] Marfai M.A., Cahyadi A., Fatchurohman H., Rosaji F.S.C., and Wibowo Y.A., "Tsunami preparedness and environmental vulnerability analysis in Kukup Beach, Gunungkidul, Indonesia," in *IOP Conference Series: Earth and Environmental Science*, 2019, vol. 256, no. 1, doi: 10.1088/1755-1315/256/1/012025.

[23] BNPB (the Indonesian National Disaster Management Agency), "Siklon Tropis Cempaka Sebabkan Banjir Longsor dan Puting Beliung," 2017. [Online]. Available: https://bnpb.go.id/siklon-tropis-cempaka-sebabkan-banjir-longsor-dan-puting-beliung-11-. [Accessed: 02-Dec-2018].

[24] BPS (The Indonesian Central Bureau for Statistics), *Arjosari Subdistrict in Numbers 2018*. Pacitan: Central Bureau for Statistics, 2018.

[25] Cian F., Marconcini M., and Ceccato P., "Normalized Difference Flood Index for rapid flood mapping: Taking advantage of EO big data," *Remote Sens. Environ.*, vol. 209, no. October 2016, 2018, pp.712-730, doi: 10.1016/j.rse.2018.03.006.

[26] USGS, "Using the USGS Landsat 8 Product," 2016. [Online]. Available: https://earthexplorer.usgs.gov/. [Accessed: 05-Aug-2018].

[27] Cortés-Ramos J., Farfán L.M., and Herrera-Cervantes H., "Assessment of tropical cyclone damage on dry forests using multispectral remote sensing: The case of Baja California Sur, Mexico," *J. Arid Environ.*, vol. 178, no. November 2019, 2020, p.104171, doi: 10.1016/j.jaridenv.2020.104171.

[28] Ho L.T.K., and Umitsu M., "Micro-landform classification and flood hazard assessment of the Thu Bon alluvial plain, central Vietnam via an integrated method utilizing remotely sensed data," *Appl. Geogr.*, vol. 31, no. 3, 2011, pp.1082-1093, doi: 10.1016/j.apgeog.2011.01.005.

[29] Ferral A., Luccini E., Aleksinkó A., and Scavuzzo C.M., "Flooded-area satellite monitoring within a Ramsar wetland Nature Reserve in Argentina," *Remote Sens. Appl. Soc. Environ.*, vol. 15, no. November 2017, 2019, p.100230, doi: 10.1016/j.rsase.2019.04.003.

[30] Khosravi K., Shahabi H., Pham B.T., Adamowski J., Shirzadi A., Pradhan B., Dou J., Ly H.B., Gróf G., Ho H.L., Hong H., Chapi K. and Prakash I., "A comparative assessment of flood susceptibility modeling using Multi-Criteria Decision-Making Analysis and Machine Learning Methods," *J. Hydrol.*, vol. 573, 2019, pp.311-323, doi: 10.1016/j.jhydrol.2019.03.073.

[31] Auynirundronkool K., Chen N., Peng C., Yang C., Gong J., and Silapathong C., "Flood detection and mapping of the Thailand Central plain using RADARSAT and MODIS under a sensor web environment," *Int. J. Appl. Earth Obs. Geoinf.*, vol. 14, no. 1, 2012, pp.245-255, doi: 10.1016/j.jag.2011.09.017.

[32] de Beurs K.M., McThompson N.S., Owsley B.C., and Henebry G.M., "Hurricane damage detection on four major Caribbean islands," *Remote Sens. Environ.*, vol. 229, no. April, 2019, pp.1–13, doi: 10.1016/j.rse.2019.04.028.

[33] BIG, "Using DEMNAS Data," 2018. [Online]. Available: http://tides.big.go.id/DEMNAS/. [Accessed: 05-Aug-2019].

[34] Holben B.N., "Characteristics of maximum-value composite images from temporal AVHRR data," *Int. J. Remote Sens.*, vol. 7, no. 11, 1986, pp.1417-1434, doi: 10.1080/01431168608948945.

[35] Hermas E.S., Gaber A., and El Bastawesy M., "Application of remote sensing and GIS for assessing and proposing mitigation measures in flood-affected urban areas, Egypt," *Egypt. J. Remote Sens. Sp. Sci.*, no. xxxx, 2020, doi: 10.1016/j.ejrs.2020.03.002.

[36] Capolongo D., Refice A., Bocchiola D.,

D'Addabbo A., Vouvalidis K., Soncini A., Zingaro M., Bovenga F., and Stamatopoulos L., "Coupling multitemporal remote sensing with geomorphology and hydrological modeling for post flood recovery in the Strymonas dammed river basin (Greece)," *Sci. Total Environ.*, vol. 651, 2019, pp.1958-1968, doi: 10.1016/j.scitotenv.2018.10.114.

[37] Chormanski J., Okruszko T., Ignar S., Batelaan O., Rebel K.T., and Wassen M.J., "Flood mapping with remote sensing and hydrochemistry: A new method to distinguish the origin of flood water during floods," *Ecol. Eng.*, vol. 37, no. 9, 2011, pp.1334-1349, doi: 10.1016/j.ecoleng.2011.03.016.

[38] Haq M., Akhtar M., Muhammad S., Paras S., and Rahmatullah J., "Techniques of Remote Sensing and GIS for flood monitoring and damage assessment: A case study of Sindh province, Pakistan," *Egypt. J. Remote Sens. Sp. Sci.*, vol. 15, no. 2, 2012, pp.135-141, doi: 10.1016/j.ejrs.2012.07.002.

[39] Marfai M.A., Sunarto., Khakim N., Cahyadi A., Rosaji F.S.C., Fatchurohman H., and Wibowo Y.A., "Topographic data acquisition in tsunami-prone coastal area using Unmanned Aerial Vehicle (UAV)," in *IOP Conference Series: Earth and Environmental Science*, 2018, vol. 148, no. 1, doi: 10.1088/1755-1315/148/1/012004.

[40] M Saharia M., Kirstetter P.E., Vergara H., Gourley J.J., and Hong Y., "Characterization of floods in the United States," *J. Hydrol.*, vol. 548, no. March, 2017, pp.524-535, doi: 10.1016/j.jhydrol.2017.03.010.

[41] Mishra K., and Sinha R., "Flood risk assessment in the Kosi megafan using multi-criteria decision analysis: A hydro-geomorphic approach," *Geomorphology*, vol. 350, 2020, p.106861, doi: 10.1016/j.geomorph.2019.106861.

[42] Das S., "Geospatial mapping of flood susceptibility and hydro-geomorphic response to the floods in Ulhas basin, India," *Remote Sens. Appl. Soc. Environ.*, vol. 14, no. January, 2019, pp.60-74, doi: 10.1016/j.rsase.2019.02.006.

[43] Zeng Z., Lan J., Hamidi A.R., and Zou S., "Integrating Internet media into urban flooding susceptibility assessment: A case study in China," *Cities*, vol. 101, no. 1037, 2020, p.102697, doi: 10.1016/j.cities.2020.102697.

[44] Bourenane H., Bouhadad Y., and Guettouche M.S., "Flood hazard mapping in urban area using the hydrogeomorphological approach: case study of the Boumerzoug and Rhumel alluvial plains (Constantine city, NE Algeria).," *J. African Earth Sci.*, vol. 160, no. December 2018, 2019, p.103602, doi: 10.1016/j.jafrearsci.2019.103602.

[45] Dimitriadis P., Tegos A., Oikonomou A., Pagana V., Koukouvinos A., Mamassis N., Koutsoyiannis D., and Efstratiadis A., "Comparative evaluation of 1D and quasi-2D hydraulic models based on benchmark and real-world applications for uncertainty assessment in flood mapping," *J. Hydrol.*, vol. 534, 2016, pp.478-492, doi: 10.1016/j.jhydrol.2016.01.020.

[46] Caletka M., Michalková M.Š., Koli M., and Trizna M., "Quality of flood extents delineated by a non-hydrodynamic GIS tool," *Catena*, vol. 175, no. September 2017, 2019, pp.367-387, doi: 10.1016/j.catena.2018.12.032.

[47] Bates P.D., and De Roo A.P.J., "A simple raster-based model for flood inundation simulation," *J. Hydrol.*, vol. 236, no. 1-2, 2000, pp.54-77, doi: 10.1016/S0022-1694(00)00278-X.

[48] Gichamo T.Z., Popescu I., Jonoski A., and Solomatine D., "River cross-section extraction from the ASTER global DEM for flood modeling," *Environ. Model. Softw.*, vol. 31, 2012, pp.37-46, doi: 10.1016/j.envsoft.2011.12.003.

[49] Leitão J.P., and de Sousa L.M., "Towards the optimal fusion of high-resolution Digital Elevation Models for detailed urban flood assessment," *J. Hydrol.*, vol. 561, no. December 2017, 2018, pp.651-661, doi: 10.1016/j.jhydrol.2018.04.043.

[50] Chen H., Liang Q., Liu Y., and Xie S., "Hydraulic correction method (HCM) to enhance the efficiency of SRTM DEM in flood modeling," *J. Hydrol.*, vol. 559, 2018, pp.56–70, doi: 10.1016/j.jhydrol.2018.01.056.